SLAC-PUB-10172

THE *BABAR* ELECTROMAGNETIC CALORIMETER IN ITS THIRD YEAR OF OPERATION

IVO GOUGH ESCHRICH

Imperial College of Science, Technology and Medicine
Blackett Laboratory, Prince Consort Road, London SW7 2BW, England
E-mail: ivo@slac.stanford.edu

(For the BABAR Collaboration)

The *BABAR* experiment at the SLAC B-Factory has recorded more than 80 fb^{-1} of integrated luminosity since 1999. Its electromagnetic calorimeter which consists of 6580 CsI(Tl) crystals has to detect both photons below 20 MeV as well as electrons in the 0.5-9 GeV range with a few percent resolution. Status and performance of the readout electronics including reliability issues and operational experience after the first three years of operation are presented.

1. Introduction

The *BABAR* detector[1] at the SLAC B-Factory has been taking data since May 1999, recording more than 80 fb^{-1} of integrated luminosity by May 2002. It is interesting at this point to review the performance of its electromagnetic calorimeter (EMC) as well as the steps that were necessary to obtain this performance. At this conference we have reported on calibration[2] of the EMC, radiation damage to its 6580 CsI(Tl) crystals[3], and extrapolations towards significantly higher luminosity[4]. This contribution will focus exclusively on the front end electronics.

The *BABAR* electromagnetic calorimeter maintains an energy resolution of a few percent over the range from 0.5 MeV to 9 GeV. At the same time it copes with the high rates of photon background at an instantaneous luminosity exceeding $4 \times 10^{33}\mathrm{cm}^{-2}\mathrm{s}^{-1}$. This is accomplished by employing an analog shaping time constant of 800 ns to lessen pileup effects, and a 3.71 MHz digital sampling rate using 10-bit ADCs. A custom range encoding curcuitry[5] preserves 18 bits of dynamic range by using four different analog amplification stages. A latched comparator curcuit is used to pick the best range, two rangebits are set accordingly, and the analog signal routed to a 10-bit ADC. These 12-bit samples of 24 channels are multiplexed into one 1.5 Gbit/s fiber

Work supported in part by the Department of Energy contract DE-AC03-76SF00515.
Stanford Linear Accelerator Center, Stanford University, Stanford, CA 94309

Presented at the 10th International Conference on
Calorimetry in High Energy Physics, Pasadena, CA, March 25-29, 2002

optic link to off-detector readout modules. Here they are converted back to the full energy range, stored in a pipeline, and copied to the first level trigger. If the latter accepts the event, the corresponding samples are read from the pipeline. Peak energy and time of the original pulse are determined ("feature extraction") and passed on to the next trigger level.

2. Feature Extraction and Digital Filter

A parabolic fit to the waveform determines the energy. The hit time is calculated from the ratio of the first to zeroth time-weighted moment of the raw waveform sum.

A matched digital filter is applied to samples of less than 30 MeV in order to reduce background and electronics noise. It achieves up to 50% reduction of total hit multiplicity under normal beam conditions. The digital filter enhances the signal-to-noise ratio for known signal shape and background characteristics. It is implemented as a linear transformation of the raw waveform given by a set of samples x_i into filtered samples $y_i = \sum_j a_j x_{i+j}$. The optimal weights a_j are determined for each crystal using clean pulse shape measurements and auto-correlation coefficients of the noise. For data taking the noise consists of constant electronics noise and beam-related background which may change its characteristics with luminosity and other beam parameters. The weights are calculated based on non-triggered waveforms and can be easily adjusted whenever necessary. For calibrating the EMC with a radioactive source[2] the weights are optimized to eliminate electronics noise.

3. Diagnostics and Monitoring

Live monitoring of currents, voltages, temperatures, etc. is provided using EPICS[6] software tools. Characteristic parameters like crystal occupancy, hit timing and multiplicity are extracted from the data as it is recorded. The shift crew is automatically alerted when a parameter drifts out of tolerance. With a few hours latency, the now fully reconstructed events provide higher-level benchmark parameters like π^0 mass and width, energy-momentum ratio, and track-cluster matching efficiency.

Daily calibrations using a lightpulser system check the complete readout path. A xenon flashlamp combined with spectral filter, attenuator, and light mixer delivers a spectrum equivalent to all but the lowest energies via optical fibers to every crystal. A reference crystal calibrated with radioactive sources provides normalization. The lightpulser system is also used to test the linearity of the electronic calibration by scanning the spectrum.

4. Readout Electronics

4.1. *Calibration*

Calibration of the readout electronics is performed by injecting a known charge into the preamplifier. Two capacitors – one small, one large – are used to cover the entire energy range. Each of the CARE chip's four amplification ranges is calibrated individually first, then a simultaneous fit is performed over all ranges which produces the lookup table for recovering the full 18-bit dynamic range out of 12-bit (10 mantissa, 2 range bits) words.

Electronic calibration data has proven to be useful to diagnose even subtle hardware defects, often down to a particular pin or solder pad.

4.2. *Electronics Noise*

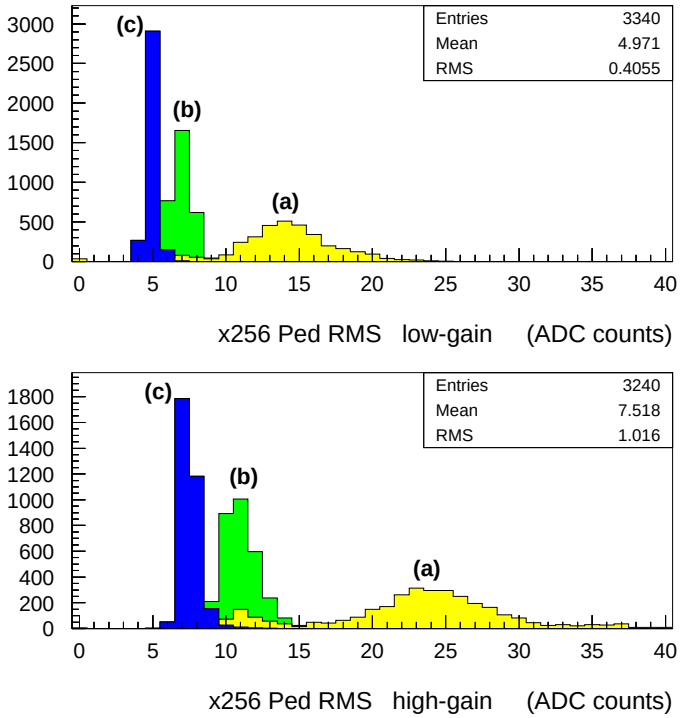

Figure 1. Distribution of raw pedestal RMS widths across the calorimeter after turn-on in May 1999 (a), after low-voltage power supplies were equipped with filters in October 1999 (b), and after correcting an unstable curcuit on the I/O Boards and raising the bias voltage to 50V in December 1999 (c).

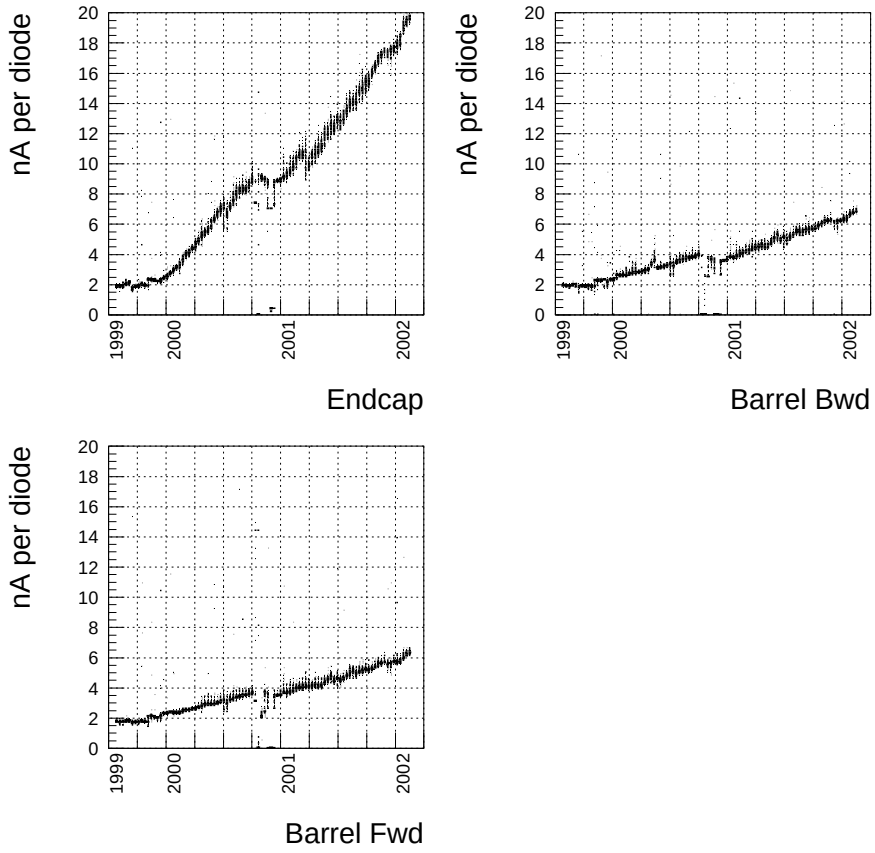

Figure 2. Average leakage current per readout diode over the period from June 1999 to March 2002.

The average electronics noise level today is equivalent to 320 keV, effectively reduced by digital filtering from 450 keV. Initially the noise level was much higher due to switching noise from the low voltage power supplies (Fig. 1). This was overcome by implementing line filters. Correcting an unstable curcuit on the I/O Board and increasing the diodes' reverse-bias voltage from 30 V to 50 V yielded another 10% improvement.

There has been no notable change in pedestal width after three years. On the other hand, the leakage current of the reverse-biased readout diodes have increased at a fast pace (Fig. 2). This effect, seen in the Belle calorimeter as well[7], is currently under investigation.

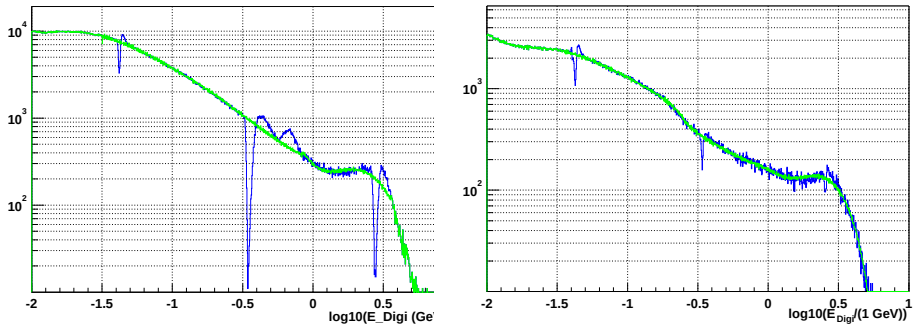

Figure 3. Energy spectrum of all channels, corrected and uncorrected, 2000 (left) and 2002 (right) data.

4.3. *Linearity*

The electronic calibration corrects nonlinearities of the preamplifier response. However, at first the EMC data still showed nonlinear behavior in certain energy windows (left of Fig. 3) which had to be corrected offline. This effect resulted from the overlay of three independent problems.

A curcuit on the ADC board could be driven into an oscillating state when the board was running under high load, for example during an electronic calibration when all channels fire simultaneously. This was the strongest contribution to the observed nonlinearity and required energy corrections of up to 10%. In the 2000/2001 winter shutdown all ADC boards were modified to remove the oscillation.

The second largest contribution ($\leq$ 4% correction) turned out to be crosstalk between neighboring channels, propagating through the preamplifier cable shields. It is now corrected for as part of the electronic calibration procedure. The crosstalk pattern was surveyed for every channel inside an ADC board and its neighboring boards during the 2000/2001 shutdown. As part of the calibration, the magnitude of the crosstalk is determined by pulsing only every other channel while reading out the crosstalk signal in the unpulsed channels. The correction is then applied to each channel's calibration according to the pattern expected for this channel, scaled with the magnitude measured as part of the same calibration.

After removing these two contributions, the EMC data was left with nonlinearities requiring corrections of up to 2%, however only in very narrow energy windows (right of Fig. 3). They appeared precisely where the range encoding curcuitry switches from one energy range to the next one. The underlying effect is still under investigation, however a correction procedure has been deployed recently which removes the nonlinearity.

4.4. *Reliability*

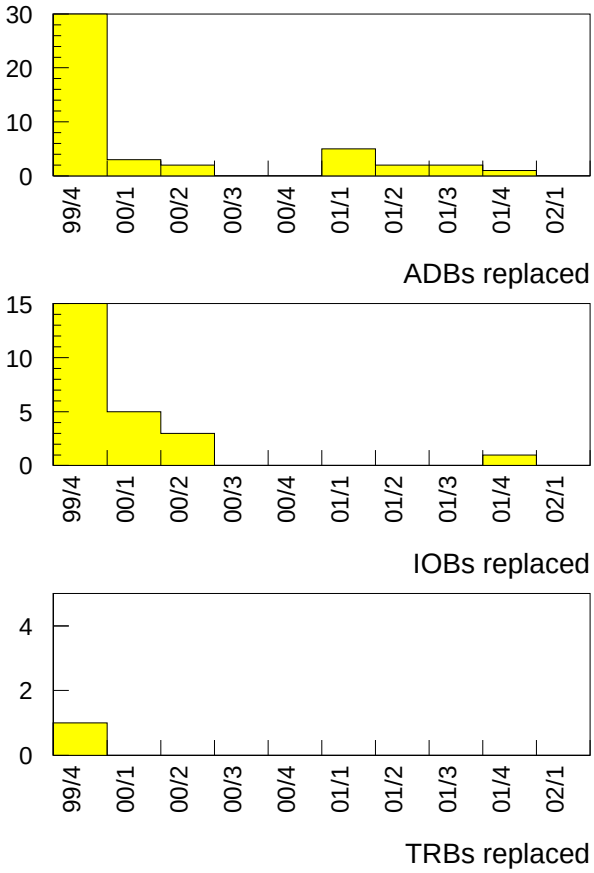

Figure 4. Number of frontend electronics board failures per quarter since October 1999, for ADC Boards (top, serves 12 channels, 560 in system), I/O Boards (center, 72 channels, 100 in system), and Transition Boards (bottom, 720 channels, 10 in system).

Only a small fraction of the electronics components – readout diodes and preamplifiers – are not easily accessible. They are implemented in twofold redundancy to allow for at least 10 years of continuous operation without any major intervention. To date, there is only one out of 6580 channels which has been unusable since installation. One of two diodes/preamplifiers has been disabled for 11 other channels.

The readily replacable components include ADC boards, I/O boards, and transition boards. While the failure rate was substantial immediately follow-

ing installation or reinstallation during a shutdown, it has subsided rapidly (Fig. 4).

In the first months of operation the fiber optics transmitters were dying at an alarming rate. It was found the vendor had supplied CD lasers, unsuited for continuous operation under *BABAR* conditions. All transmitters were replaced with vertical cavity surface emitting lasers from a different vendor. After an initial infant mortality of 1% in the first two weeks there has been no failure since.

The most common failure modes observed on front end electronics boards so far were, in descending order of occurrence:

(1) Multipin connectors where one or many pins were disconnected from their solder pads. This was mostly due to the combination of weak solder joints and mechanical stresses from (un)plugging the connector, or bad alignment of the connector and its counterpart. Reinforcing the solder joints and fixing the alignment remedied this problem completely.
(2) Unstable electrical contacts due to faulty solder joints. As was the case above, cold solder joints were a frequent flaw of the manufacturing process, and were easily fixed by resoldering the contact.
(3) Failures of individual electronic components, apart from the fiber optics transmitters described earlier, have been limited to a few instances with no particular pattern as to the type of component involved.

5. Conclusion

In its first three years of operation, the *BABAR* electromagnetic calorimeter has overcome a number of initial surprises and teething pains. It is now running in a most stable fashion, with little need for maintenance.

References

1. B. Aubert *et al.* [*BABAR* Collaboration], The *BABAR* detector, Nucl. Instr. Meth. **A479**, 1 (2002), SLAC-PUB-8569, hep-ex/0105044.
2. M. Kocian, these proceedings.
3. T. Hryn'ova, these proceedings.
4. W. Wisniewski, these proceedings.
5. D. R. Freytag and G. Haller, Analog Floating-Point BiCMOS Sampling Chip and Architecture of the Babar CsI Calorimeter Front-End Electronics System at the SLAC B-Factory, *BABAR*-Note-285; IEEE Trans.Nucl.Sci.43:1610-1614,1996.
6. `http://www.aps.anl.gov/epics/`
7. B. Shwartz, these proceedings.